Journal of Archaeological Science: Reports 27 (2019) 101929

Contents lists available at ScienceDirect

Journal of Archaeological Science: Reports

journal homepage: www.elsevier.com/locate/jasrep

Molecular and isotopic analyses on prehistoric pottery from the *Virués-Martínez* cave (Granada, Spain)

Eloisa Manzano[a,*], Alejandra García[b], Samuel Cantarero[a], David García[c], Antonio Morgado[b], Jose Luis Vílchez[a]

[a] Department of Analytical Chemistry, University of Granada, E-18071 Granada, Spain
[b] Department of Prehistory and Archaeology, University of Granada, E-18071 Granada, Spain
[c] Institute of Mediterranean and Near Eastern Languages and Cultures, Spanish National Research Council (CSIC), E-28037 Madrid, Spain

ARTICLE INFO

Keywords:
Gas chromatography–mass spectrometry
Isotope-ratio mass spectrometry
Ultra-performance liquid chromatography-high resolution mass spectrometry
Archaeological organic residues

ABSTRACT

The analysis of the organic residues in archaeological pottery usually involves the use chromatography and mass spectrometry techniques. The identification of organic compounds processed in archaeological vessels, which generally degrade over archaeological timescales, provides insights about their origin and uses of the vessels. This paper provides an advance of archaeometric characterization of the organic residues in seventeen pottery vessels from the end of the 4th millennium BCE found in the *Virués-Martínez* cave (Granada, Spain), using gas chromatography–mass spectrometry (GC–MS), gas chromatography-isotope ratio mass spectrometry (GC-C-IRMS), and ultra-performance liquid chromatography-high resolution mass spectrometry (UPLC-HRMS). To our knowledge this is the first study on the use of UPLC-HRMS on archaeological residues. Despite the fact that the identification of plant remains continues to be elusive, this study demonstrates the potential usefulness of UPLC-HRMS technique to study the polar fraction of plant residues, thus allowing us to formulate more specific hypotheses about the vegetal compounds that have survived in association with the pottery vessels (erucamide, matricarin, piptamine, piceatannol). Our results indicate that the occupants of the cave used the vessels to process plant materials and also degraded animal fats (ruminant fat) and it is very likely that the vessels were used for a variety of purposes, with accumulation of by-products over time, and were not made exclusively for funerary practices. The $\delta^{13}C$ values C16:0 and C18:0 fatty acids obtained open a debate on the consumption of dairy compounds in the Iberian Peninsula during the end of the Neolithic and beginning of the Copper Age.

1. Introduction

Pottery has a great potential to inform the study of human societies in the past. Several approaches have been used, but the analysis of organic residues has been one of the most important cornerstones of this interdisciplinary research field over the last decades. The main goal of any Organic Residue Analysis (ORA) is to identify the original organic contents of the vessel in order to understand the dietary habits, rituals and burial ceremonies, trade customs, treatment of human diseases and pharmaceutical knowledge of the people who occupied an archaeological site.

The development of advanced analytical instrumentation and improved analytical procedures has enabled the growth of research linked to the archaeological study (Roffet-Salque et al., 2015; Roffet-Salque et al., 2017). Gas chromatography coupled to mass-spectrometry (GC–MS) (Heron et al., 1991; Evershed, 2008; Craig et al., 2012; Manzano et al., 2015; Heron et al., 2016; Mayyas et al., 2017; Reber et al., 2018), gas chromatography-isotope ratio mass spectrometry (GC-IRMS) (Mottram et al., 1999; Craig et al., 2005; Colombini et al., 2005; Spangenberg et al., 2006), high-performance liquid chromatography (HPLC), high-performance liquid chromatography–atmospheric pressure chemical ionization-mass spectrometry (HPLC–APCI-MS) (Saliu-Modugno et al., 2011), and high performance liquid chromatography-electrospray ionization- quadrupole time of flight mass spectrometry (HPLC-ESI-QToF) (Parras et al., 2015) have been recently used for the analysis of lipids in archaeometry. Ultra-Performance Liquid Chromatography-High Resolution Mass Spectrometry (UPLC-HRMS) has been widely used to identify organic compounds in different matrices such as soils, biological fluids, food, water, and others. Despite its advantages and multiple uses, this technique has not been fully developed for use in archaeological samples, and there are only a few articles available (Manzano et al., 2015; Tuñón-López et al., 2017). A recent study on the

* Corresponding author.
E-mail address: emanzano@ugr.es (E. Manzano).

https://doi.org/10.1016/j.jasrep.2019.101929
Received 11 April 2019; Received in revised form 25 June 2019; Accepted 29 June 2019
Available online 22 July 2019
2352-409X/

presence of triacylglycerols and sterols in archaeological pottery have used ultra-high-performance liquid chromatography-atmospheric pressure chemical ionization-high resolution mass spectrometry (UHPLC-APCI-HRMS) and UPLC/HRMS-based metabolomics to investigate the biodeterioration of archaeological materials (Tuñón-López et al., 2017).

The number of analytical studies conducted on organic residues from ceramic vessels found in the Iberian Peninsula is limited. However, some of the studies available have demonstrated the relationship between pottery vessels from the Neolithic period and dairy products (Martí et al., 2009) and animal fats (Sánchez et al., 1998) stored or processed in the vessels. Analyses on pottery beakers from the Copper Age have identified beer (Guerra, 2006), pear juice, animal fats and dairy products (Rojo et al., 2008). Analyses on pottery vessels from the Argaric settlement of Peñalosa (Jaén, Spain), dating from the Bronze Age, revealed the presence of ruminant (ovine or bovine) and non-ruminant (porcine and equine) tissues, vegetable oils, waxes, conifer resins and grape seeds (Manzano et al., 2015). Dairy products, cereals and animal fat were also identified by GC–MS in vessels from the late Bronze Age (Guerra et al., 2011–12).

This paper reports the results of the ORA in pottery vessels from the *Virués-Martínez* cave (Granada, Spain) that date back to the end of the 4th millennium BCE. Some of the vessels contained charcoal fragments, seeds, bones or stones and samples from the interior of the vessels were taken for chemical analysis in order to establish the functionality of the vessels. The results of the ORA are presented in this paper. A suite of analytical techniques including GC–MS, GC-C-IRMS and UPLC-HRMS has been used for the determination of organic residues in early Copper Age vessels from the *Virués-Martínez* cave in southern Spain.

2. Historical background

The *Virués-Martínez* cave is located in the Sierra Elvira Mountains, in the municipality of Atarfe nearby the city of Granada (Southern Spain) (Fig. 1). The cave was named after speleologists Gustavo Virués Ortega and José Antonio Martínez Jiménez, who died in the Atlas Mountains (Morocco) in the spring of 2015. Members of the Iliberis Caving Club discovered the cave while conducting an inspection of the area. The entrance to the cave was blocked by natural processes until its recent discovery. The *Virués-Martínez* cave is like a "time capsule" of the early Copper Age burial practices and the archaeological deposit is currently preserved in situ.

The geological context of the site is Sierra Elvira mountain system which comprises the southernmost part of the Middle Sub-Baetic system in the outer regions of the Baetic mountain range. Sierra Elvira is composed of calcareous rocks of marine origin deposited during the Mesozoic era around 200 to 145 million years ago. The action of groundwater flowing along tectonic fractures was responsible for the formation of the subterranean system of which the *Virués-Martínez* cave is part of.

The cave has a length of 140 m and a maximum depth of 18.5 m from the entrance. It cannot be affirmed that the current entrance was the primary entrance to the cave: in fact, access to the cave requires caving equipment. The cave has a series of chambers where the archaeological remains were found in an astonishing degree of preservation and arranged around the cave as the prehistoric communities had left them. The cave may have been used for burial rituals by the presence of remains of human bones and related grave goods like pottery vessels and large flint blades. These burials customs has been documented in other archaeological contexts inside caves in southern Iberia (Vera, 2014: 122).

In order to date the occupation of the cave, the morphological features of these vessels and flint blades were compared with the morphology of archaeological materials found in related sites in the south of the Iberian Peninsula.

Some of the bowls found in the cave were carinated shapes, which may be ascribed to the end of 4th millennium BCE and first quarter of 3th millennium BCE (Martínez, 2013: 100).

Similar vessels with globular forms and the carinated shapes have also been found in other sites such as Los Millares (Almería, Spain), Polideportivo de Martos (Jaén, Spain), Papauvas (Huelva, Spain), and Torre de San Francisco (Badajoz, Spain) dated in the same period. The flint blades found in the *Virués-Martínez* cave show morphological features related with the production of these artefacts in the Copper age in the Iberian Peninsula (Morgado and Pelegrin, 2012).

Other archaeological sites (burials in caves, megalithic tombs and pits) dating from the end of the 4th millennium BCE and 3rd

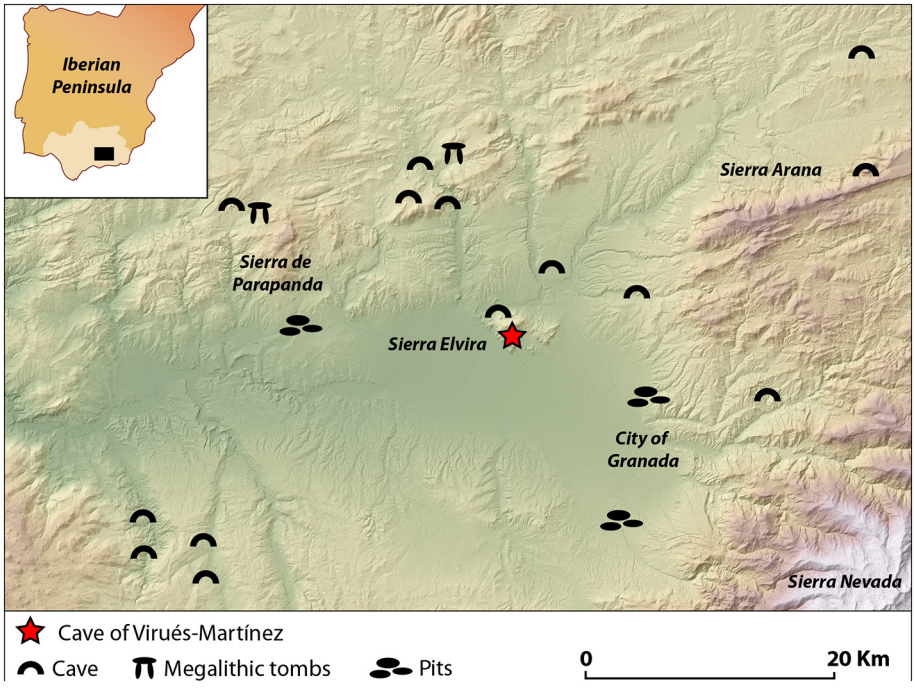

Fig. 1. Location of the *Virués-Martínez* cave and archaeological sites nearby with evidences of burial rituals.

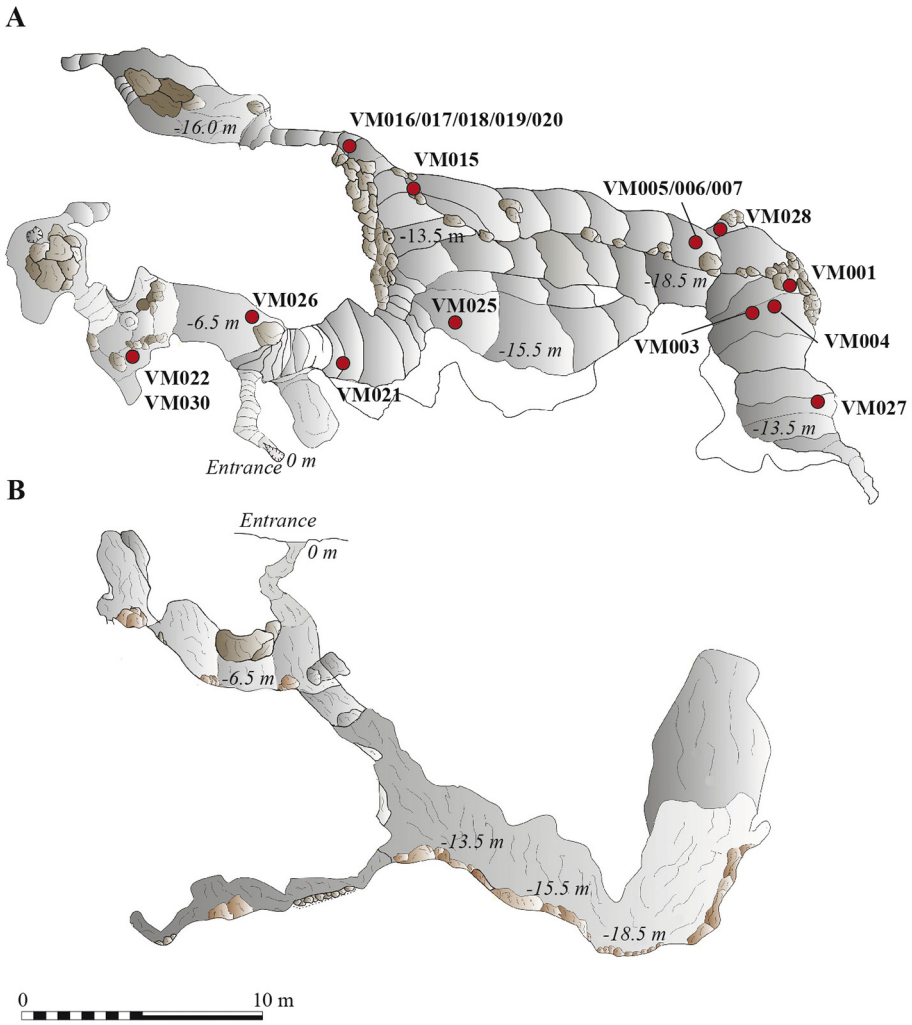

Fig. 2. *Virués-Martínez* cave plan. Pottery vessels location. A. Map view. B. Cross-section view.

millennium BCE have been found near the *Virués-Martínez* cave (Fig. 1).

3. Material and methods

3.1. Description of potteries

When the cave was discovered, the pieces were arranged around different areas of the cave (Fig. 2). Different groups of vessels were identified according to their shape (small vessels, carinated bowls, pots and globular-shaped vessels) and potential use. Several pieces had small handles and the surfaces of the vessels were burnished (García et al., 2017) (Fig. 3).

3.2. Sampling and sample handling

The analytical balance used to weight all the samples was Balance XS105DU (Mettler Toledo, Greifensee, Zurich, Switzerland). The analysis of the pottery found in the *Virués-Martínez* cave was conducted according to the principles set in Organic Residue Analysis (ORA), Guidance for Good Practice (Dunne, 2017). To prevent the introduction of contaminants the vessels were handled with silk nitrile gloves and immediately wrapped in aluminium foil. To avoid the loss of soluble residue components all the vessels remained unwashed. After visual inspection, 17 samples were selected as representative of the different groups of vessels based on their shape and specific functions. No visible residues were adhered to the surface of the vessels but the organic components that absorbed into the clay matrix were investigated as they can be preserved over many centuries. Samples were removed from the inner surfaces of each vessel using an electric drill (Dremel) with a tungsten carbide bit. Sampling was done by first removing the outermost layer of ceramic, to prevent contamination. Each sample was crushed and ground into powder in an agate mortar, and accurately weighed and collected before the GC–MS, GC–C–IRMS and UPLC-HRMS analysis.

For GC–MS, the following amounts of fine powder from each of the 17 samples were weighed and analysed: VM001 (1.003 g), VM003 (1.031 g), VM004 (1.012 g), VM005 (1.087 g), VM006 (1.080 g), VM007 (1.049 g), VM015 (0.710 g), VM016 (1.009 g), VM017 (1.002 g), VM018 (1.015 g), VM019 (1.001 g), VM020 (1.009 g), VM021 (1.047 g), VM022 (1.013 g), VM025 (1.015 g), VM027 (1.016 g) and VM028 (0.765 g). GC–C–IRMS was only applied to samples VM019 and VM021 due to the no availability of sample powder. Similarly, UPLC-HRMS was applied to samples VM019 (0.933 g), VM020 (1.033 g), VM021 (1.035 g) and VM025 (1.002 g).

In order to ensure that no contamination was introduced during the preparation procedure, two soil samples from the cave (1.100 and 1.090 g) were considered blank samples (VM-S1 and VM-S2) and were analysed with the samples.

3.3. Sample treatment

A modified GC–MS extraction procedure (Evershed et al., 1990) was

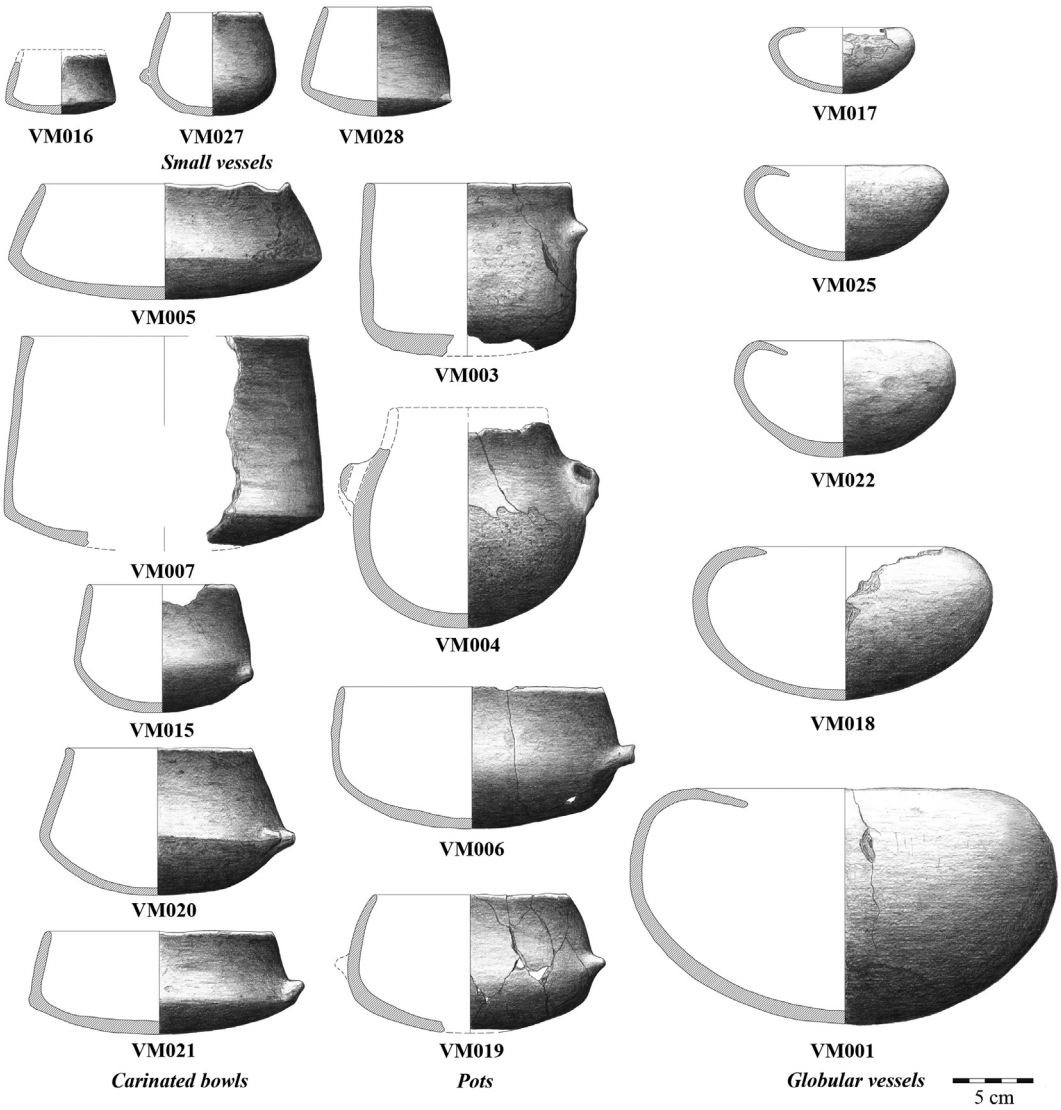

Fig. 3. Typology of the pottery vessels found in the *Virués-Martínez* cave: small vessels, carinated bowls, pots and globular-shaped vessels.

performed using 15 mL dichloromethane: methanol (2:1 *v*/v) as solvent. For the extraction of lipids, fatty acids and other compounds, the ceramic powder was sonicated twice for 15 min (5133 JP Selecta, Barcelona, Spain) and centrifugated at 3500 rpm for 5 min. The two extracted liquids were dried in a nitrogen atmosphere at 50–60 °C. Prior to injection into the chromatograph a derivatization reaction was performed with 500 µL of hexane and 37.5 µL of 3-trifluoromethylphenyl trimethylammonium hydroxide dissolved in 5% methanol as derivatization reagent. The reaction was carried out in the ultrasonic bath and took 30 min at ambient temperature. This derivatization is based on a procedure used for characterization of drying oils in paintings that was developed by our research team and successfully tested in previous studies (Manzano et al., 2011). Prior to the GC–MS analysis, a measured amount of internal standard (C13 n-alkane) was added to each sample. Finally, 2 µL of the derivatized samples were injected into the chromatograph.

The UPLC-HRMS extraction procedure was similar to the GC procedure but in order to identify polar compounds, a mixture of methanol:water (70,30 *v*/v) with 0.1% of HCl was used as solvent. Finally, 10 µL of the samples was injected into the liquid chromatograph and analysed by HRMS.

3.4. Analytical techniques

The organic composition of residues in pottery was obtained by GC–MS, GC-C-IRMS, and UPLC-HRMS. GC–MS analyses were carried out on an Agilent 6890 N gas chromatograph system (Agilent Technologies, Palo Alto, CA, USA) coupled to an Agilent 5973 N mass spectrometer (Agilent Technologies, Palo Alto, CA, USA). The GC was fitted with an automatic injector (model 7683) and automatic sample tray (model 7683). An HP-5MS capillary column (30 m × 0.25 mm × 0.25 µm particle size) was used. Samples (2 µL) were injected using splitless injector at 250 °C. The oven was initially held at 70 °C for 2 min, ramped at 12 °C min^{-1} to 250 °C, and finally increased to 290 °C at 20 °C min^{-1} and held for 8 min. The mass spectrometer was operated with an ionization potential of 70 eV and mass spectra were collected by scanning over the range *m/z* 50–520 uma. Instrumental parameters were optimized as described previously (Manzano et al., 2015). Peak assignments were performed on the basis of the analysis of available standard compounds and comparing their mass spectra with those from the Wiley Mass Spectral Library.

A Thermo Delta V Advantage coupled to a Thermo Trace GC Ultra Gas Chromatograph was used for IRMS detection (ThermoFisher Scientific, Waltham, MA). A Conflo IV system was the interface and the reactor temperature (Cu–Ni–Pt) was set at 1000 °C. The mass

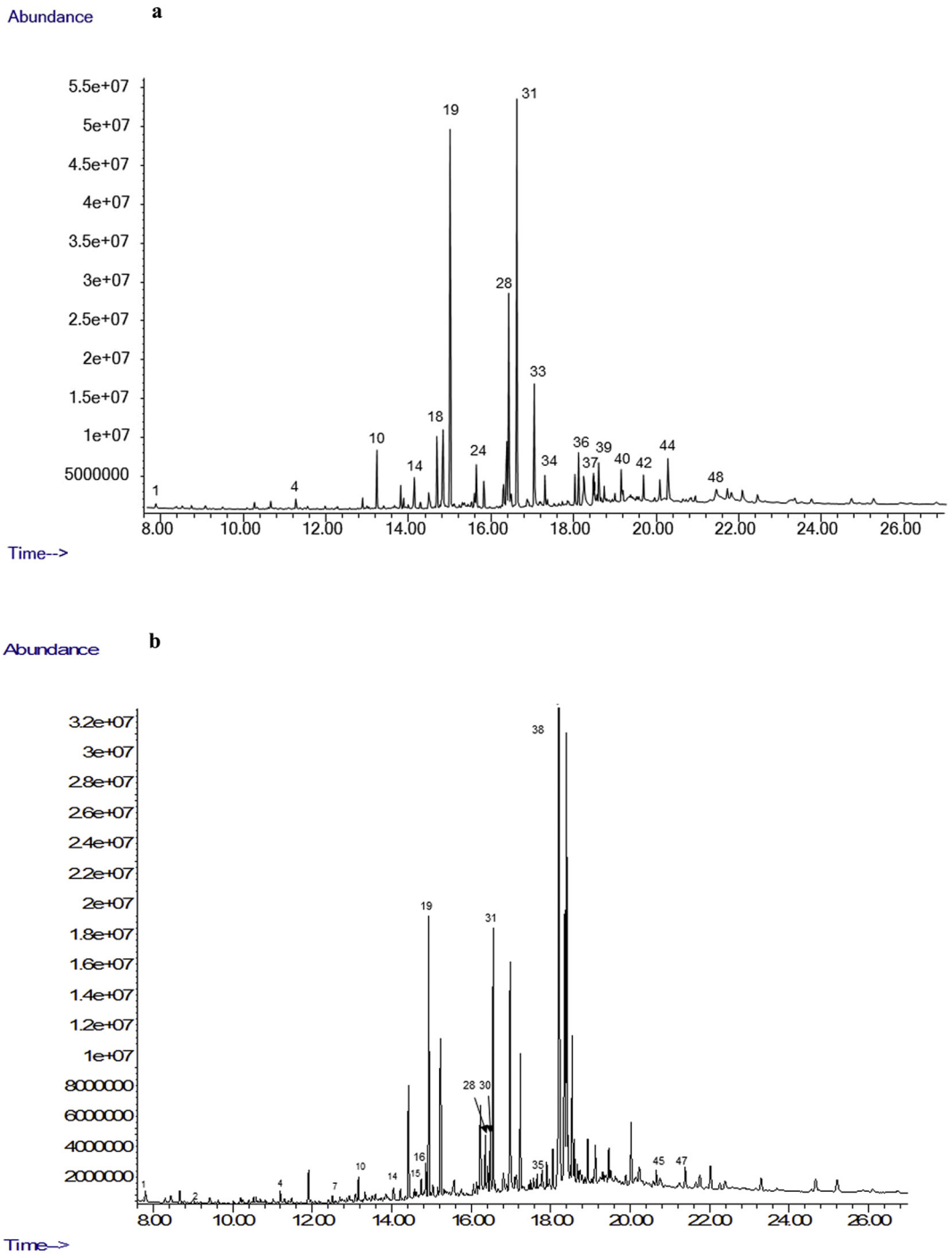

Fig. 4. Chromatograms from a) VM019 and b) VM 016.
1 (C9:0); 2 (C10:0); 4 (C12:0); 10 (C14:0); 14 (C15:0); 18 (C16:1(n-9 Z)); 19 (C16:0); 24 (C17:0); 28 (C18:1(n-9 Z)); 30 (octadecanenitrile); 33 (C22H46); 34 (C19:0); 35 (C23H48); 36 (C20:0); 37 (C21:0); 38 (9-octadecenamide); 39 (C20H42); 40 (C22:0); 42 (C23:0); 44 (C24:0); 45 (C28H58); 47 (C29H60); 48 (C26:0).

spectrometer source pressure was 1.9 × 10–06 mbar. The GC was fitted with an HP-1 column (30 m × 0.25 mm ID × 0.25 μm). The carrier gas was helium and the GC oven was programmed at 70 °C for 2 min, ramped at 12 °C min^{-1} to 250 °C, and finally increased to 290 °C at 20 °C min^{-1} and held for 8 min. Carbon isotope ratios are reported in the standard delta notation relative to the Pee Dee Belemnite (PDB) standard. The results were expressed as $\delta^{13}C$ (%) = [(Rsample − Rstandard) / Rstandard], where R is $^{13}C/^{12}C$ in per mil. To obtain accurate and reproducible $\delta^{13}C$ values, triplicate injections were performed for each sample. CO_2 gas of a known isotopic composition was used as working reference standard. Mass balance corrections were made for the methyl group added during the methylation process: $\delta^{13}C_{sample} = (29 \times \delta^{13}C_{measured} - \delta^{13}C_{meoh})/28$, where $\delta^{13}C_{meoh}$. 1σError, based on repeated analysis of an external fatty acid methyl ester (FAME) standard through the sample runs, was 0.2‰.

UPLC–HRMS analysis was performed on a Waters Acquity UPLC™ H-Class system (Waters, Manchester, UK), consisting of an ACQUITY UPLC™ binary solvent manager and an ACQUITY UPLC™ sample manager. An ACQUITY UPLC HSS T3™ column (1.8 μm, 2.1 mm × 100 mm) (Waters, UK) was used for the separation of compounds. A Synap G2 quadrupole tandem time of flight (QTOF) mass spectrometer (Waters), equipped with an orthogonal Z-spray™ electrospray ionization (ESI)

source was used for the determination of molecular formulae. Chromatographic separation was done with a binary gradient mobile phase consisting of 0.5% (*v*/v) aqueous acetic acid solution (solvent A) and acetonitrile (solvent B). The flow rate was 400 μL min^{-1}, the column was kept at 40 °C, and the injection volume was 10 μL. Gradient conditions were as follows: initial mobile phase 95% (A), which was linearly decreased to 0% (A) within 15.0 min and held for 1.0 min in order to maintain the column using 100% organic mobile phase. Finally, back to 100% in 0.1 min and held for 1.9 min to equilibrate the column. Total run time was 18.0 min.

The QTOF mass spectrometer was operated with ESI in positive and negative ion mode. The QTOF parameters were optimized in order to obtain the maximum accuracy in mass molecular formulae determination. The main mass spectrometer parameters were: capillary voltage, 2.8 kV; cone voltage, 25.0 V; source temperature, 100 °C; desolvation temperature, 500 °C; cone gas flow, 40 Lh^{-1}; desolvation gas flow, 800 Lh^{-1}. Nitrogen (99.995%) was used as cone and desolvation gas. The working mass range was between 50.0 uma and 1200.0 uma in positive mode.

4. Results

4.1. GC–MS and GC-C-IRMS results

Lipids absorbed onto pottery vessels were extracted according to the methodology described above. The chromatographic results showed that lipid preservation was similar in the 17 analysed samples. The values of Total Lipid Extract (TLE) were between 104 and 240 μg·g^{-1}, that is > 5 μg·g^{-1} in all the samples. The analysis revealed no significant peaks in the blank samples.

GC–MS revealed the presence of common contaminants in archaeological sites such as phthalate plasticisers from plastic bags. In particular 1,2-benzenedicarboxylic acid, diethyl ester (ethyl phthalate) (m/z = 222), 1,2-benzenedicarboxylic acid, dibutyl ester (butyl phthalate) (m/z = 278) and 1,2-benzenedicarboxylic acid, bis(2-ethylhexyl) ester (bis(2-ethylhexyl) phthalate) (m/z = 390) were present in almost all samples analysed. Nevertheless the chemical profiles of these compounds are easily identifiable and do not prevent the correct interpretation of analytical data. Thus, in order to simplify the results they were removed from the chromatograms and tables. No significant amounts of cholesterol or squalene were identified in the residue or soil samples analysed. The comparison of lipids absorbed onto the vessels (once the outermost layer was removed) with blank samples using GC–MS suggested that the environmental and/or burial contamination did not affect the interpretation of the residue chromatograms.

The 17 samples analysed yielded good chromatograms after the extraction and derivatization of the lipid content from the vessels. The lipid distribution was similar for all the samples: LCFAs (long-chain fatty acids), n-alkanes, n-alkanols and unsaturated FAs (fatty acids). Fig. 4 shows two representative chromatograms (VM019 and VM 016). All the compounds separated and identified from the samples are listed in Table 1 (compounds #1 to #51); their time of retention (tR) and mass-to-charge ratio (m/z) are also shown.

In order to facilitate the interpretation of the original content of the vessels, the identified compounds were grouped by chemical category (see Table 2). The compounds found at higher concentrations are in bold. The 17 pottery pieces were classified according to their shape and potential intended use into the following four groups: vessels (VM016, VM027 and VM028), carinated bowls (VM005, VM007, VM015, VM020 and VM021), pot-shaped vessels (VM003, VM004, VM006 and VM019), and globular-shaped vessels (VM001, VM017, VM018, VM022 and VM025).

Palmitic (C16:0) and stearic (C18:0) methyl esters were the dominant components in all the samples. Table 2 also shows the estimated C18:0/C16:0 and C18:1/C16:0 ratios, although they do not provide unequivocal information regarding the origin of the lipid components.

Table 1
Compounds identified in the 17 samples by GC–MS. The compounds identified in each of the 17 samples are specified at the bottom of the table.

#	tR	m/z	Identified compound
1	7.800	172	Nonanoic acid, methyl ester
2	8.996	186	Decanoic acid, methyl ester
3	11.010	194	1,4-Benzenedicarboxylic acid, dimethyl ester
4	11.192	214	Dodecanoic acid, methyl ester
5	11.207	214	Undecanoic acid, 10-methyl-, methyl ester
6	12.207	228	Tridecanoic acid, methyl ester
7	12.509	226	Dihydro methyl jasmonate
8	12.812	242	Tridecanoic acid, 12-methyl-, methyl ester
9	12.964	268	Pentadecane, 2,6,10,14-tetramethyl
10	13.161	242	Tetradecanoic acid, methyl ester
11	13.812	256	Methyl 13-methyltetradecanoate
12	13.903	282	Hexadecane, 2,6,10,14-tetramethyl
13	13.918	296	9-Octadecenoic acid (*Z*)-, methyl ester
14	14.069	256	Pentadecanoic acid, methyl ester
15	14.569	210	1-Pentadecene
16	14.615	270	Pentadecanoic acid, 14-methyl-, methyl ester
17	14.751	237	Hexadecanenitrile
18	14.766	268	9-Hexadecenoic acid, methyl ester, (Z)
19	14.933	270	Hexadecanoic acid, methyl ester
20	15.008	292	Methyl-3-(3,5-ditertbutyl-4-hydroxyphenyl) propionate
21	15.160	226	Hexadecane
22	15.523	284	Hexadecanoic acid, 14-methyl-, methyl ester
23	15.569	282	Nonadecane
24	15.750	284	Heptadecanoic acid, methyl ester
25	16.129	280	Cycloeicosane
26	16.144	252	1-Octadecene
27	16.311	294	9,12-Octadecadienoic acid (Z,Z)-, methyl ester
28	16.356	296	9-Octadecenoic acid (Z), methyl ester
29	16.401	296	9-Octadecenoic acid (E), methyl ester
30	16.417	265	Octadecanenitrile
31	16.553	298	Octadecanoic acid, methyl ester
32	16.977	255	Hexadecanamide
33	17.098	310	Docosane
34	17.295	312	Nonadecanoic acid, methyl ester
35	17.780	324	Tricosane
36	17.962	326	Eicosanoic acid, methyl ester
37	18.552	340	Heneicosanoic acid, methyl ester
38	18.598	309	9-Octadecenamide, *N*,*N*-dimethyl ester
39	18.931	282	Eicosane
40	19.082	354	Docosanoic acid, methyl ester
41	19.461	366	Hexacosane
42	19.628	368	Tricosanoic acid, methyl ester
43	20.037	380	Heptacosane
44	20.218	382	Tetracosanoic acid, methyl ester
45	20.658	394	Octacosane
46	20.885	396	Pentacosanoic acid, methyl ester
47	21.400	408	Nonacosane
48	21.658	410	Hexacosanoic acid, methyl ester
49	23.688	438	Heptacosanoic acid, 25-methyl-, methyl ester
50	23.703	438	Octacosanoic acid, methyl ester
51	26.302	298	1-Eicosanol

VM001: 1; 4;7; 10;17;19;24;28;30;31;35;36;39.
VM003: 1;4;7;9;10;12;14;16;19;24;26;27;28;31;36;39;40;42;48.
VM004: 1;4;7,10;17;19;23;28;30;31;35;36;39;41;48;50.
VM005: 1;4;7;10;14;19;24;28;30;31;35;38;39.
VM006: 1;2;4;5;7;10;14;17;19;23;25;28;30;31;35;38;39;40.
VM007: 1;2;4;7;10;14;16;18;19;22;25;28;30;31;35;38;39;41.
VM015: 1;2;4;7;10;14;16;18;19;22;24;27;28;30;31;33;35;36;39;40;41;44.
VM016: 1;2;4;7;10;14;15;16;19;28;30;31;35;38;39;45;47.
VM017: 1;2;4;10;14;16;17;19;23;24;28;30;31;38;39.
VM018: 1;2;4;7;10;14;17;19;22;28;30;31;35;36;38;39;40;43;44;48;49;51.
VM019:
1;2;3;4;6;8;10;11;13;14;16;18;19;22;23;24;27;28;31;36;37;39;40;42;44;46;48.
VM020: 1;2;4,7;10;14;16;17;19;31;32;34;36;39.
VM021: 1;4;7;16;19;24;28;30;31;36;40;44;47;48;49.
VM022: 4;10;17,19;21;28;30;31;36;36;39;40;43.
VM025: 1;2;4;7;10;14,17;19,20;23;24;28,30;31;33,36;39,47.
VM027: 1;2;4;10;14,16;18;19;22;28;29;31;36;38;40;48.
VM028: 1;2;4;7;10;14;16;17,19;22;28;30;31;36;38;39;40;41;44;48.

Table 2
Compounds identified in each sample classified into categories. Highest concentrations are in bold. Cx:y refers to fatty acids with carbon number (x) and number of unsaturations (y). C15H29N, C16H31N, C17H33N, C18H35N (penta, hexa, hepta, octadecanenitrile); C16H33NO (hexadecanamide); C20H39NO (9-octadecenamide); C13H22O3 (dihydromethyljasmonate); C18H28O3 (methyl3-(3,5-di-tert-butyl-4-hydroxyphenyl)propionate); HC15br (2,6,10,14-tetramethyl); HC16br (2,6,10,14-tetramethyl); C11:0br (10-methyl); C13:0br (12-methyl); C14:0br (13-methyl); C15:0br (14-methyl); C16:0br (14-methyl); C27:0br (25-methyl); C20H420 (1-eicosanol); C18H34O2 (methyl 8-(2-hexylcyclopropyl)octanoate); C10H10O4 (1,4-benzene dicarboxylic acid, dimethyl ester); C14H22O (p-(1,1,3,3-tetramethylbutyl)phenol); C15H30, C18H36 (1-penta,1-octadecene); C20H40 (1-eicosene); C16H34, C17H36, C18H38, C19H40 (hexa, hepta, octa, nonadecane); C20H42 (eicosane); C22H46, C23H48, C25H52, C26H54, C27H56, C28H58, C29H60 (doco, tri, penta, hexa, hepta, octa, nonacosane).

		VM01	VM017	VM018	VM022	VM025	VM03	VM04	VM06	VM019
Saturated fatty acid	Short-chain	**C9:0**	C9:0	C9:0	C12:0	C9:0	C9:0	C9:0	C9:0	C9:0
		C10:0	C10:0	C10:0	C14:0	C10:0	C12:0	C12:0	C10:0	C10:0
		C14:0	C12:0	C12:0	**C16:0**	C12:0	**C14:0**	C14:0	C12:0	C12:0
		C16:0	**C14:0**	C14:0	**C18:0**	**C14:0**	**C16:0**	**C16:0**	C14:0	**C14:0**
		C18:0	**C16:0**	**C16:0**		**C16:0**	**C18:0**	**C18:0**	**C16:0**	**C16:0**
			C18:0	**C18:0**		**C18:0**			**C18:0**	**C18:0**
	Odd-chain	C17:0	C15:0	C15:0		C15:0	**C15:0**		C15:0	**C15:0**
						C17:0	C17:0			C17:0
	Long-chain	C20:0		C20:0	C20:0	C20:0	**C20:0**	C20:0	C23:0	C20:0
				C22:0	**C22:0**		**C22:0**	**C26:0**		**C21:0**
				C24:0			C23:0	C28:0		**C22:0**
				C26:0			C26:0			**C23:0**
										C24:0
										C25:0
										C26:0
Branched-chain fatty acids			C15:0br	C15:0br			**C15:0br**		C11:0br	C13:0br
			C16:0br	C16:0br						C14:0br
				C27:0br						**C15:0br**
										C16:0br
Unsaturated fatty acid		**C18:1(Z)**	**C18:1(Z)**	**C18:1(Z)**	**C18:1(Z)**	**C18:1(Z)**	**C18:1(Z)**	**C18:1(Z)**	C18:1(Z)	**C16:1**
							C18:1(E)			C18:1(Z)
							C18:2(Z,Z)			**C18:2(Z,Z)**
Saturated hydrocarbons		**C20H42**	**C20H42**	C23H48 **C25H52 C27H56**	C16H34	**C19H40**	**C22H46**	**C19H40**	**C19H40**	C20H42
					C20H42	C20H42	C23H48	C23H48	**C20H42**	
					C23H48	**C22H46**	C26H54	**C25H52**	**C23H48**	
					C27H56	**C29H60**		**C29H60**		
Unsaturated hydrocarbons				**C20H40**			C18H36		C20H40	
							C20H40			
Branched-chain hydrocarbons							HC15br			
							HC16br			
Nitriles		**C16H31N**	C15H29N	C15H29N		**C15H29N**		**C16H31N**	**C15H29N**	
		C18H35N	C18H35N	C17H30N		C18H35N		C18H35N	C18H35N	
9-Octadecenamide			**C20H39NO**						**C20H39NO**	
Amides				**C20H39NO**						
Others		C13H22O3		**C20H420**	C14H22O	C13H22O3	C13H22O3	C13H22O3	C13H22O3	**C18H34O2**
				C13H22O3			C18H28O3			C10H10O4
C16:0/C18:0		0.91	1.57	2.26	0.83	1.26	0.46	1.15	0.78	1.19
C18:1/C16:0		0.28	0.19	0.21	0.30	0.33	0.87	0.36	0.36	0.49

		VM05	VM07	VM015	VM020	VM021	VM016	VM027	VM028
Saturated fatty acid	Short-chain	C9:0	C9:0	C9:0	C9:0	C9:0	C9:0	C9:0	C9:0
		C12:0	C10:0	C10:0	C10:0	C12:0	C10:0	C10:0	C10:0
		C14:0	C12:0	C12:0	C12:0	**C16:0**	C12:0	C12:0	C12:0
		C16:0	**C14:0**	**C14:0**	C14:0	**C18:0**	C14:0	**C14:0**	C14:0
		C18:0	**C16:0**	**C16:0**	**C16:0**		**C16:0**	**C16:0**	**C16:0**
			C18:0	**C18:0**	**C18:0**		**C18:0**	**C18:0**	**C18:0**
	Odd-chain	C15:0	C15:0	**C15:0**	C15:0			C15:0	C15:0
		C17:0		C17:0	C19:0				
	Long-chain			**C20:0**	C20:0	C20:0		C20:0	C20:0
				C22:0		**C22:0**		**C22:0**	**C22:0**
				C24:0		**C24:0**			**C24:0**
						C26:0			C26:0
Branched-chain fatty acids			C15:0br	C15:0br	C15:0br	C15:0br	C15:0br	**C15:0br**	C15:0br
			C16:0br	C16:0br		C16:0br	C16:0br	C16:0br	C16:0br
Unsaturated fatty acid		C18:1(Z)	C16:1	C16:1			**C18:1(Z)**	**C16:1**	**C18:1(Z)**
			C18:1(Z)	**C18:1(Z)**				**C18:1(Z)**	
				C18:2(Z,Z)				**C18:1(E)**	
Saturated hydrocarbons		**C20H42**	**C20H42**	**C22H46**	**C20H42**		C17H36		C18H38
		C23H48	C26H54	**C23H48**			**C23H48**		**C25H52**
				C25H52			**C25H52**		
							C28H58		
							C29H60		
Unsaturated hydrocarbons			C18H36		C20H40		C15H30		
Branched-chain hydrocarbons									
Nitriles		C18H35N	C18H35N	C18H35N	C16H31N	C18H35N	C18H35N		C18H35N

(*continued on next page*)

Table 2 (*continued*)

	VM05	VM07	VM015	VM020	VM021	VM016	VM027	VM028
9-Octadecenamide	**C20H39NO**	**C20H39NO**				**C20H39NO**		
Amides				**C16H33NO**			**C20H39NO**	**C20H39NO**
Others	C13H22O3	C13H22O3	C13H22O3	C13H22O3	C13H22O3	C13H22O3		C13H22O3
C16:0/C18:0	1.20	1.62	0.96	0.71	1.07	0.84	1.34	1.09
C18:1/C16:0	0.42	0.38	0.45	–	0.28	0.34	0.38	–

In residues from samples VM001, VM003, VM006, VM015, VM016, VM020 and VM022, C18:0 was slightly more abundant than C16:0 (C16:0/C18:0 ≤ 1), while in the remaining ten samples C16:0 was slightly more abundant, suggesting an animal origin for fats extracted from the first seven vessels cited (Evershed et al., 1997; Dudd and Evershed, 1998; Kimpe et al., 2004). A particularly high content of C16:0 was found in the VM018 residue. The identification of other compounds will be discussed below. However, other species detected in the chromatograms could not be specifically identified (assignment lower than 90%) by comparing with the verified reference spectra from the NIST Mass Spectral Library. The identification of these compounds would require further analysis and they have not been included in the table. For some selected samples, the GC–MS studies were complemented with GC-C-IRMS and UPLC-HRMS analyses.

Table 2 shows the abundance of odd, even and branched-chain saturated fatty acids (C9:0–C26:0) and unsaturated fatty acids (C16:1, C18:1, C18:2) in 16 of the 17 samples. The presence of methyl-branched fatty acids (MBFAs) has been typically linked to bacterial sources (Hauff and Vetter, 2009). Polyunsaturated fatty acid (C18:2) was also detected in high concentrations in samples VM003 and VM019 from the pot-shaped group and in sample VM015 from the carinated group. In addition, small to trace amounts of short-chain fatty acids (C9:0, C10:0, C12:0 and C14:0) were found in the 17 samples analysed, except in VM022 vessel. These acids are common components of animal fat (degraded dairy fats) (Spangenberg et al., 2006). The presence of the mixture of positional isomers of 9-octadecenoic acid (C18:1 [Z] and C18:1 [E]) identified in samples VM003 and VM027 suggests a monogastric or non-ruminant origin (Evershed et al., 1997). Long-chain fatty acids in combination with unsaturated fatty acids in high proportions suggest the presence of plant and animal-derived fats, the latter probably coming from ruminants feeding on a plant-based diet (Halmemies-Beauchet-Filleau et al., 2014). Odd long-chain alkanes present in plant leaf waxes and beeswax were detected in many samples, often in high concentrations (Table 2). The source of these compounds cannot be clearly identified but long-chain fatty acids in combination with unsaturated fatty acids and hydrocarbons are consistent with their being used in these vessels. Additionally, the significant content of eicosanol in sample VM018 and of C24:0 in samples VM015, VM018, VM019, VM021 and VM028 suggests the some kind of waxy materials in these vessels. Similar results supporting this suggestion have been reported previously (Regert et al., 2001; Evershed, 2008; Maia and Nunes, 2013; Roffet-Salque et al., 2015). Phenolic content (28-ol) in sample VM018 and n-nonacosane in VM016, VM021 and VM025 can be attributed to plants related to the genus *Brassica* (Cartea et al., 2011).

Odd-chain fatty acids (C15:0–C17:0) and branched-chain fatty acids (C13:0br–C16:0br) were present in most of the samples analysed which can be explained by the fact that decomposition of the organic matter preserved in pottery is largely accomplished by bacteria during deposition (Hauff and Vetter, 2009). These acids may have a ruminant origin or their presence may be due to microbial contamination (Mottram et al., 1999; Dudd et al., 1999). Consequently, the results need to be interpreted in conjunction with the compound specific isotopic analysis of organic residues in selected samples VM019 and VM020. The most abundant fatty acids, octadecanoic (C18:0) and hexadecanoic (C16:0), were then classified according to their carbon isotopic composition using GC-C-IRMS. Table 3 shows the $\delta^{13}C$ values. Carbon isotopic composition of stearic acid ($\delta^{13}C18:0$) versus palmitic acid ($\delta^{13}C16:0$) of modern animal and plant fats and oils from Europe (Dudd and Evershed, 1998; Kimpe et al., 2004; Spangenberg et al., 2006) were used as reference samples and used for comparison with the $\delta^{13}C$ values of the VM020 sample ($\delta^{13}C18:0 = -33.995‰$; $\delta^{13}C16:0 = -30.484‰$). The $\delta^{13}C$ values fall within the ruminant dairy fat cluster in the $\delta^{13}C16:0$ vs $\delta^{13}C18:0$ plot (Fig. 5). The results can also be plotted as $\Delta^{13}C$ vs $\delta^{13}C_{16:0}$ (where $\Delta^{13}C = \delta^{13}C_{18:0} - \delta^{13}C_{16:0}$). The value obtained for VM020 residue (−3.511) plots in the area for ruminant milk fats (Evershed et al., 2008; Copley et al., 2005) and as such is consistent with animals fed on C3 plant diets, isotopically representative of the archaeological period (Bender, 1971). The results also suggest the presence of adipose fat for carbon isotopic signatures where $\Delta^{13}C$ is lower than −3.3‰, a value generally related to milk fats (Craig et al., 2012). The isotope values plotted for sample VM019 ($\delta^{13}C18:0 = -26.904‰$; $\delta^{13}C16:0 = -28.402‰$) (Table 3) were not clear but the residues seem to contain a mixture of ruminant and non-ruminant fats (Fig. 5). Nevertheless, the $\Delta^{13}C$ value (−1.498) against $\delta^{13}C_{16:0}$ plots in the cluster for ruminant adipose fat (Evershed et al., 2008). These data indicate that the animals consumed a mainly C3 plant diet (Bender, 1971). Fig. 5-b supports ruminant dairy fats (VM019 sample) (Saliu-Modugno et al., 2011).

Table 3
GC-C-IRMS measurements of duplicated VM19 and VM020 samples. Carbon isotopic composition of carbon ($^{13}C/^{12}C$ isotopic composition of the palmitic/stearic acids ratio) was expressed as $\delta^{13}C$ value in ‰ vs. Vienna Pee Dee Belemnite limestone standard (VPDB).

Sample	$\delta^{13}C/\delta^{12}C$			
		C16:0		C18:0
VM019		−26.87		−28.42
		−26.91		−28.42
		−26.94		−28.36
	Average	−26.90	Average	−28.40
	SD	0.04	SD	0.04
VM020		−30.52		−34.08
		−30.44		−33.95
		−30.49		−33.96
	Average	−30.48	Average	−34.00
	SD	0.04	SD	0.08

In addition, Nitrogen-derived compounds (C15H29N, C16H31N, C17H30N, C18H35N) were identified by GC–MS on the surface layer of most vessels. The occurrence of alkyl nitriles has been attributed to the burning of organic matter containing alkyl amides (Simoneit et al., 2003). The presence of alkyl amides (C16H33NO, C20H39NO) in the residues could be explained by reactions between fatty acids and ammonia naturally occurring during biomass burning. Although the origin of these compounds in the *Virués-Martínez* cave should be further investigated, emissions from meat grilling have been reported as source of alkyl nitriles and alkyl amides (Rogge et al., 1991).

4.2. UPLC-HRMS results

Complementary information from UPLC–HRMS helped in the interpretation of the results. UPLC-HRMS analysis was used to determine the molecular formula of the compounds adsorbed to samples VM019,

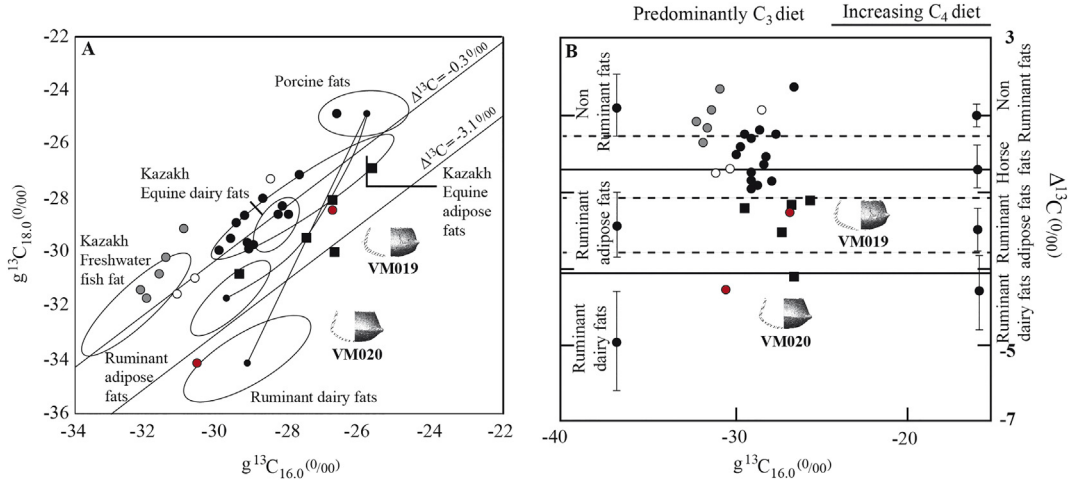

Fig. 5. Scatterplots of (a) $\delta^{13}C$ values of C16:0 fatty acid against the C18:0 fatty acid extracted from modern reference fats as reference samples (Mileto et al., 2017) and (b) $\delta^{13}C$ values of C16:0 against the $\Delta^{13}C$ values ($\delta^{13}C18:0–\delta^{13}C16:0$).

VM020, VM021 and VM025. Fig. 6 shows the chromatograms of a blank and sample VM020 obtained by UPLC-HRMS. The mass spectrum profile was obtained in positive ion mode, using Leu-enkephalin and Sodium formate as internal and external standard for HRMS calibration. The molecular formulas are listed in Table 4. In addition, the table shows the precursor ion and major and minor fragments found for the proposed structures. One or more major fragments and several minor fragments were identified for all compounds. Therefore, the identification was based not only in the precursor ion but also in the presence of major and minor fragment ions, which helped in the identification. Since the chromatograms of blank samples show no peaks, it is assumed that all the detected peaks are attributed to the samples.

Accurate mass measurements and fragment patterns were used for structure confirmation. $C_{22}H_{43}NO$ (accurate mass: 338.3411) was detected in all the samples analysed and was identified as erucamide, a fatty acid amide usually present in plant root exudates and cereal (Lu et al., 2014). In VM020 and VM021 samples, piptamine and *o*-demethyl forbexanthone have been attributed to $C_{23}H_{41}N$ (accurate mass: 332.3317) and $C_{18}H_{14}O_6$ (accurate mass: 327.0869), respectively. Piptamine, produced by *Piptoporus betulinus* fungus, grows on birch trees and has been used for its medicinal properties for millennia. *O*-demethyl forbexanthone is found in *Rheedia brasiliensis* trees (Meighan et al., 1958). In VM020 sample, piceatannol (3,3′,4′,5-tetrahydroxy-trans-stilbene) is the proposed compound for the molecular formula $C_{14}H_{12}O_4$ (accurate mass: 245.0805). Piceatannol is a natural stilbene polyphenol occurring in a number of plant species, including grapes (*Vitis vinifera*), and has been reported to exhibit anticancer and anti-inflammatory properties (Bavaresco et al., 2002) (Matsui et al., 2010). In VM021 sample, matricarin is the proposed compound attributed to $C_{17}H_{20}O_5$ (accurate mass: 277.1804), a sesquiterpene found in the essential oil obtained from *Matricaria chamomilla*.

5. Discussion

A total of 17 pottery vessels (small vessels, carinated bowls, pots and globular-shaped pieces) were recovered from the *Virués-Martínez* cave. The discrimination of the source of compounds identified represents a challenge mainly due to the lack of specific biomarkers (Evershed, 2008) and to degradation during cooking processes. Few chemical fingerprints have been found in the residues that provide evidence of past human activity in the *Virués-Martínez* cave. Nevertheless, the molecular and isotopic studies revealed no significant migration of lipids from the surrounding soil to the buried potsherds. GC screening revealed few signs of oxidative damage and extremely good preservation of unsaturated fatty acids, high abundances of short-chain fatty acids. The absence of dicarboxylic acids that are coming from the degradation of unsaturated fatty acids reinforce the excellent conservation state of the organic residues. Waterlogging and extreme desiccation may preserve residues in burial environments. The presence of alkanoic acids (C16:1, C18:1, C18:2) found in most of the archaeological residues analysed could be supported by the absence of oxidative environment in the cave.

The combination of GC–MS and GC-IRMS information allows the confirmation of the residues broadly resembling mixture of animal fats and vegetal matter preserved inside the vessels. Based on the alkanoic distribution pattern it is not possible to understand the origin of the vegetal and animal fats identified in the residues, but probably the vessels had multiple uses, with accumulation of by-products over time, before being deposited as burial goods. In ten of the 17 analysed samples, C16:0 was more abundant than C18:0 (C16:0/C18:0 > 1), which is indicative of vegetal oil. Since fatty acids are susceptible to oxidative degradation, the ratios showed in Table 1 (C16:0/C18:0 and C18:1/C16:0) have been interpreted with caution.

Additionally, a high abundance of odd, even and branched-chain saturated fatty acids (C9:0-C26:0) is observed in practically all samples. Linear odd-chain and branched-chain fatty acids are one of the main degradation products of the fermentation of dietary carbohydrates in the rumen (Baeten et al., 2013). Microbial contamination could also be the source of odd and branched-chain fatty acids owing to the prolonged contact of the residues with soil organic matter (Mottram et al., 1999; Dudd et al., 1998).

On the other hand, no remains of animal processing were detected from the analysis of surrounding soil and migration or leaching of lipids from the soil to the buried vessels was shown to be negligible.

The fatty acids of low molecular weight (C9:0–C14:0) occurring in most of the archaeological samples analysed are common components of degraded milk fat (Copley et al., 2005). Indeed, ruminant milk fats were the dominant type of fat found in residues from vessels from all the phases of the Neolithic (Smyth and Evershed, 2015). However, the attribution of the fat source based on the detection of short chain fatty acids is still open to discussion. The isotopic analyses on sample VM020 are consistent with the presence of dairy fat. In VM019 sample, the source of fatty acids remains unclear as the results plot between the non-ruminant and ruminant adipose fat clusters.

In addition, lignoceric acid (C24:0) and/or C21, C22, C23, C25, C28 hydrocarbons were found in some of the residues extracted from pottery vessels of different shapes. In addition to lignoceric acid (C24:0), eicosanol was also identified in VM018 sample, a globular-shaped vessel. Waxy residues could be suggested in some vessels, particularly in those where animal fat was also identified. The detection of dairy

Fig. 6. Blank (1) and VM20 (2) archaeological samples obtained by UPLC-HRMS.

product residues would have explained the presence of waxy materials as this may have been used to waterproof the inside of vessels for handling low-lipid content liquids (Rojo et al., 2008). Phenolic content (28-ol) and n-nonacosane in some residues can be attributed to Brassica vegetables (Cartea et al., 2011). No characteristic terpenoid biomarkers in degraded resins were found.

Unsaturated fatty acids (C16:1, C18:1, C18:2) and fatty acid of high molecular weight (C20:0–C26:0) identified by GC–MS suggest the handling of vegetable oil. The highest levels of C18:2 and C18:1 isomers found have been related to the presence of some kind of cereal (Evershed et al., 1997) and supported by the results from the UPLC-HRMS analyses. From the molecular formula identified by HRMS, the identified compounds were components of cereal, an essential oil and a fungus. The high levels of C18:0 and C18:1 in sample VM003 suggest the presence of degraded residues of large herbivore meat cooked with plants and large herbivore bone marrow.

No relationships were found between the presence of specific markers and vessel shape and therefore between shape and function, as has been reported in the literature (Rice, 2015).

Information from other archaeological contexts from the Neolithic and Copper Age from the Iberian Peninsula was used for the interpretation of the chemical results. The presence of beeswax in Copper Age vessels in the Iberian Peninsula has been documented previously (Rojo et al., 2008) and the analysis of 6000 potsherds from different archaeological sites in Europe, North Africa and Near East revealed that the exploitation of bee products started 9,000 years ago (Roffet-Salque et al., 2015). In the 130 fragments analysed for this study no remains of beeswax were found probably due to the poor preservation of this compound. Despite this, evidence of the exploitation of honey in the Iberian Peninsula has been documented in the form of rock art (Dams, 1983). Regarding animal fat in vessels, its presence has been documented in archaeological sites in the Iberian Peninsula (Manzano et al., 2015), sometimes related to burial contexts, like the megalithic tomb of *Monte de Os Escurros* (Pontevedra, Spain) (Prieto et al., 2005). As for dairy products, some studies have reported the presence of traces in archaeological sites of the Iberian Peninsula (Manzano et al., 2015) in Neolithic (Martí et al., 2009) and Copper Age contexts (Rojo et al., 2008), sometimes also related to burial contexts. A painted carinated-

Table 4
Proposed identification of polar compounds from archaeological samples obtained by UPLC-HRMS with molecular formula, precursor ions, product ions and proposed fragmentation of the mass spectra and tandem mass spectra for all the identified species.

MF	Sample	$[M + H]^+$ or $[M-H]^-$	ppm
$C_8H_9N_7$	VM19, VM20	204.0999	1.0
$C_{21}H_{37}N$	VM19, VM20	304.3004	4.3
$C_{24}H_{43}N_5$	VM19, VM20, VM21, VM25	402.3583	3.7
$C_{22}H_{43}NO$	VM19, VM20, VM21, VM25, VM26	338.3411	3.5
$C_8H_4O_3$	VM19, VM20, VM21, VM 25	149.0229	4.4
$C_{32}H_{17}N_{21}O_9$	VM19	840.1533	2.1
$C_{17}H_{36}N_2O$	VM19	283.2710 $[M-H]^-$	3.8
$C_{10}H_{10}O_6$	VM20	227.0590	1.5
$C_{19}H_{26}O_{10}$	VM20	415.1651	4.3
$C_{14}H_{12}O_4$	VM20	245.0805	3.7
$C_{18}H_{14}O_6$	VM20, VM21, VM25	327.0869	2.1
$C_{23}H_{41}N$	VM20, VM21	332.3317	1.8
$C_{17}H_{24}O_3$	VM21	277.1804	3.2
$C_{17}H_{20}O_5$	VM21	305.1337	2.2
$C_{40}H_{25}N_9O_{13}$	VM25	840.1650	1.8

vessel with incised decoration dating from the end of the 5th millennium BCE was found next to the head of a body in a burial site in Segudet (Andorra) (Martí et al., 2009; Guerra et al., 2011–12). A study on 2000 potsherds from different archaeological sites in the Near East concluded that the consumption of dairy products was common in the Neolithic communities of the 7th millennium BCE (Evershed et al., 2008). In Europe there are studies about the consumption of milk by the first agricultural communities (Evershed et al., 2008; Salque et al., 2013). Some studies conclude that the domestication of the animals was initially focussed on the exploitation of milk rather than meat (Vigne and Helmer, 2007). The remains in the vessels from the *Virués-Martinez* cave are consistent with the results obtained from other archaeological sites about the consumption of dairy products in the Iberian Peninsula during the Neolithic and Copper Age.

Signs of fire were also observed on the outermost surface samples VM005, VM006, VM015, VM019, VM020 and VM021, supporting that they were used for cooking. Nevertheless, it is very difficult to distinguish if the presence of signs of fire is evidence of cooking practices or the result of pottery production process, or even from both sources. Markers from food in contact with very high temperatures such as polycyclic aromatic hydrocarbons (PAHs) have been not identified in any residue. The pyrolysis of proteinaceous materials promotes the formation of nitrogen derivatives and the occurrence of alkyl nitriles has been attributed to burning of organic matter containing alkyl amides (Simoneit et al., 2003). N-containing compounds identified by GC–MS in residues (hexa-, octa-decanenitrile) supported by the UPLC-HRMS results (C8H9N7, C21H37N, C24H43N5, C23H41N) suggest complex reactions taking place during long periods of heating (cooking) on an open fire, but this cannot be confirmed. On the other hand, bacterial proteins in the rumen involved in heat treatments (cooking or roasting of protein foods) produce N-compounds derivatives (even humic acid) (Zang et al., 2000). The presence of erucamide (13-docosenamide) and oleamide (9-octadecenamide) in archaeological residues has been related to chemical contamination but it has also been reported in some oils and in emissions from meat cooking/grilling (Rogge et al., 1991). The no significant alkyl amides content in the two blank soil samples analysed suggests that the presence of these compounds in some of the vessel samples is related to reactions of fatty acids with ammonium salts from protein decomposition during burning and other combustion processes carried out inside the vessels (Wang et al., 2017).

6. Conclusions

GC–MS, GC-C-IRMS and UPLC-HRMS analyses were performed for identification of the organic residues extracted from the pottery vessels recovered from the *Virués-Martínez* cave. To our knowledge, despite the benefits and multiple uses of UPLC-HRMS, this is the first report on the use of this technique on archaeological residues. The results show the potential usefulness of UPLC-HRMS techniques to complement the study of the polar fraction of the residues, thus allowing a deep profiling of the organic residues that should be integrated with faunal, archaeobotanical and zooarchaeological evidence. Our results showed evidence of the presence of vegetal oils in all samples analysed and of fatty acids compatible with ruminant fat (possibly dairy fat) in some of the samples. It is very likely that the vessels had a multi-functional use and were not made exclusively for funerary practices. Consequently, the accumulation of by-products formed over time may explain the presence of the different residues identified. In addition, no relations were observed between the residue content and vessel shapes; therefore, vessel typology does not seem to be related to the functions or use of the pieces.

Knowledge about the functions of the vessels may shed light on the daily activities of prehistoric communities, agriculture and livestock, food consumption, as well as burial practices. In the present study, all these activities are interrelated in the symbolic practices of the prehistoric communities at the end of the 4th millennium BCE. The analysis of the vessel contents, traces of exposures to fire, erosion of the rim show that the vessels were used for cooking and food consumption before being used as burial goods.

The pottery vessels found were complete and the lack of archaeological materials from later periods indicates that the cave may have been sealed at prehistoric time. This, together with the environmental conditions of the cave, has allowed the preservation of samples for different analyses. Finally, the stratigraphy of the cave has not been altered by anthropic factors. For these reasons, the *Virués-Martínez* cave offers a great potential for research and can provide elements for debate regarding funerary rituals of the prehistoric communities in the late 4th and early 3rd millennium BCE in the south of the Iberian Peninsula in a way that can be contrasted with megalithic tombs.

Acknowledgements

This paper is dedicated to the memory of Gustavo Virués Ortega and José Antonio Martínez Jiménez. We want to acknowledge the efforts of the Iliberis Caving Club members in the preservation of the cave. This research has been supported by the Regional Government of Andalucía (Junta de Andalucía) (FQM 338) and the R & D Project HAR2015-66009-P funded by the Spanish Ministry of Economy and Competitiveness. A. García acknowledges support from a FPU 13/02389 grant from the Spanish Ministry of Education.

References

Baeten, J., Jervis, B., De Vos, D., Waelkens, M., 2013. Molecular evidence for the mixing of meat, fish and vegetables in Anglo-Saxon coarseware from Hamwic, UK. Archaeometry 55 (6), 1150–1174. https://doi.org/10.1111/j.1475-4754.2012.00731.x.

Bavaresco, L., Fregoni, M., Trevisan, M., Mattivi, F., Vrhovsek, U., Falchetti, R., 2002. The occurrence of the stilbene piceatannol in grapes. Vitis-geilweilerhof 41 (3), 133–136.

Bender, M.M., 1971. Variations in the $^{13}C/^{12}C$ ratios of plants in relation to the pathway of photosynthetic carbon dioxide fixation. Phytochemistry 10 (6), 1239–1244. https://doi.org/10.1016/S0031-9422(00)84324-1.

Cartea, M.E., Francisco, M., Soengas, P., Velasco, P., 2011. Phenolic compounds in Brassica vegetables. Molecules 16 (1), 251–280. https://doi.org/10.3390/molecules16010251.

Colombini, M.P., Modugno, F., Ribechini, E., 2005. Organic mass spectrometry in archaeology: evidence for Brassicaceae seed oil in Egyptian ceramic lamps. J. Mass Spectrom. 40 (7), 890–898. https://doi.org/10.1002/jms.865.

Copley, M.S., Berstan, R., Mukherjee, A.J., Dudd, S.N., Straker, V., Payne, S., Evershed, E.R., 2005. Dairying in antiquity. III. Evidence from absorbed lipid residues dating to the British Neolithic. J. Archaeol. Sci. 32 (4), 523–546. https://doi.org/10.1016/j.jas.

2004.08.006.
Craig, O.E., Chapman, J., Heron, C., Willis, L.H., Bartosiewicz, L., Taylor, G., Collins, M., 2005. Did the first farmers of central and eastern Europe produce dairy foods? Antiquity 79 (306), 882–894. https://doi.org/10.1017/S0003598X00115017.
Craig, O.E., Allen, R.B., Thompson, A., Stevens, R.E., Steele, V.J., Heron, C., 2012. Distinguishing wild ruminant lipids by gas chromatography/combustion/isotope ratio mass spectrometry. Rapid Commun. Mass Spectrom. 26 (19), 2359–2364. https://doi.org/10.1002/rcm.6349.
Dams, L.R., 1983. Abeilles et recolte du miel dans l'art rupestre du Levant espagnol. Homenaje al prof. vol. I Martín Almagro, Madrid.
Dudd, S.N., Evershed, R.P., 1998. Direct demonstration of milk as an element of archaeological economies. Science 282, 1478–1481. https://doi.org/10.1126/science.282.5393.1478.
Dudd, S.N., Regert, M., Evershed, R.P., 1998. Assessing microbial lipid contributions during laboratory degradations of fats and oils and pure triacylglycerols absorbed in ceramic potsherds. Org. Geochem. 29 (5–7), 1345–1354. https://doi.org/10.1016/S0146-6380(98)00093-X.
Dudd, S.N., Evershed, R.P., Gibson, A.M., 1999. Evidence for varying patterns of exploitation of animal products in different prehistoric pottery traditions based on lipids preserved in surface and absorbed residues. J. Archaeol. Sci. 26 (12), 1473–1482. https://doi.org/10.1006/jasc.1998.0434.
Dunne, J., 2017. Organic Residue Analysis and Archaeology Guidance for Good Practice. Historic England.
Evershed, R.P., 2008. Organic residue analysis in archaeology: the archaeological biomarker revolution. Archaeometry 50 (6), 895–924. https://doi.org/10.1111/j.1475-4754.2008.00446.x.
Evershed, R.P., Heron, C., Goad, L.J., 1990. Analysis of organic residues of archaeological origin by high-temperature gas chromatography and gas chromatography-mass spectrometry. Analyst 115 (10), 1339–1342. https://doi.org/10.1039/AN9901501339.
Evershed, R.P., Mottram, H.R., Dudd, S.N., Charters, S., Stott, A.W., Lawrence, G., Reeves, V., 1997. New criteria for the identification of animal fats preserved in archaeological pottery. Naturwissenschaften 84 (9), 402–406. https://doi.org/10.1007/s001140050417.
Evershed, R.P., Payne, S., Sherratt, A.G., Copley, M.S., Coolidge, J., Urem-Kotsu, D., Kotsakis, K., Özdoğan, M., Özdoğan, A., Nieuwenhuyse, O., Akkermans, P.M., Bailey, D., Andeescu, R.R., Campbell, S., Farid, S., Hodder, I., Yalman, N., Özbaşaran, M., Biçakci, E., Garkinfel, Y., Levy, T., Burton, M.M., 2008. Earliest date for milk use in the Near East and southeastern Europe linked to cattle herding. Nature 455, 528–531. https://doi.org/10.1038/nature07180.
García, D., Morgado, A., García, N., Fernández, S., Lahoz, S., Morillas, J., Lozano, J.A., Rodríguez, D., 2017. La cueva sepulcral de Virués-Martínez (Atarfe) en el contexto funerario de finales del IV milenio Cal. B. C. de la Depresión de Granada. Antiqvitas 29, 17–37.
Guerra, E., 2006. Sobre la función y el significado de la cerámica campaniforme a la luz de los análisis de contenidos. Trab. Prehist. 63 (1), 69–84.
Guerra, E., Delibes, G., Rodríguez, J.A., Crespo, M., Gómez, A., Herrán, I., Tresserras, J., Matamala, J.C., 2011–12. Residuos de productos lácteos y de grasa de carne en dos recipientes cerámicos de la Edad del Bronce del Valle Medio del Duero. BSAA Arqueol. 105–137 LXXVII-LXXVIII.
Halmemies-Beauchet-Filleau, A., Vanhatalo, A., Toivonen, V., Heikkilä, T., Lee, M.R.F., Shingfield, K.J., 2014. Effect of replacing grass silage with red clover silage on nutrient digestion, nitrogen metabolism, and milk fat composition in lactating cows fed diets containing a 60:40 forage-to-concentrate ratio. J. Dairy Sci. 97 (6), 3761–3776. https://doi.org/10.3168/jds.2013-7358.
Hauff, S., Vetter, W., 2009. Quantification of branched chain fatty acids in polar and neutral lipids of cheese and fish samples. J. Agric. Food Chem. 58 (2), 707–712. https://doi.org/10.1021/jf9034805.
Heron, C., Evershed, R.P., Goad, L.J., 1991. Effects of migration of soil lipids on organic residues associated with buried potsherds. J. Archaeol. Sci. 18, 641–659. https://doi.org/10.1016/0305-4403(91)90027-M.
Heron, C., Shoda, S., Barcons, A.B., Czebreszuk, J., Eley, Y., Gorton, M., Nishida, Y., 2016. First molecular and isotopic evidence of millet processing in prehistoric pottery vessels. Sci. Rep. 6, 38767. https://doi.org/10.1038/srep38767.
Kimpe, K., Drybooms, C., Schrevens, E., Jacobs, P.A., Degeest, R., Waelkens, M., 2004. Assessing the relationship between form and use of different kinds of pottery from the archaeological site Sagalassos (southwest Turkey) with lipid analysis. J. Archaeol. Sci. 31 (11), 1503–1510. https://doi.org/10.1016/j.jas.2004.03.012.
Lu, Y., Zhou, Y., Nakai, S., Hosomi, M., Zhang, H., Kronzucker, H.J., Shi, W., 2014. Stimulation of nitrogen removal in the rhizosphere of aquatic duckweed by root exudate components. Planta 239 (3), 591–603. https://doi.org/10.1007/s00425-013-1998-6.
Maia, M., Nunes, F.M., 2013. Authentication of beeswax (Apis mellifera) by high-temperature gas chromatography and chemometric analysis. Food Chem. 136 (2), 961–968. https://doi.org/10.1016/j.foodchem.2012.09.003.
Manzano, E., Rodriguez-Simón, L.R., Navas, N., Checa-Moreno, R., Romero-Gámez, M., Capitan-Vallvey, L.F., 2011. Study of the GC–MS determination of the palmitic–-stearic acid ratio for the characterisation of drying oil in painting: La Encarnación by Alonso Cano as a case study. Talanta 84 (4), 1148–1154. https://doi.org/10.1016/j.talanta.2011.03.012.
Manzano, E., García, A., Alarcón, E., Cantarero, S., Contreras, F., Vílchez, J.L., 2015. An integrated multianalytical approach to the reconstruction of daily activities at the Bronze Age settlement in Peñalosa (Jaén, Spain). Microchem. J. 122, 127–136. https://doi.org/10.1016/j.microc.2015.04.021.
Martí, B., Capel, J., Juan, J., 2009. Una forma singular de las cerámicas neolíticas de la Cova de l'Or (Beniarrés, Alicante): los vasos con asa-pitorro. In: De la Mediterranée et d'ailleurs, Melanges offerts à Jean Guilaine. Archives d'Écologie Prèhistorique, Toulouse, pp. 463–482.
Martínez, R.M., 2013. El IV milenio ANE en el Guadalquivir Medio, BAR International Series 2563. Archeopress, Oxford.
Matsui, Y., Sugiyama, K., Kamei, M., Takahashi, T., Suzuki, T., Katagata, Y., Ito, T., 2010. Extract of passion fruit (Passiflora edulis) seed containing high amounts of piceatannol inhibits melanogenesis and promotes collagen synthesis. J. Agric. Food Chem. 58 (20), 11112–11118. https://doi.org/10.1021/jf102650d.
Mayyas, A.S., Khrisat, B.R., Hoffmann, T., El Khalili, M.M., 2017. Fuel for lamps: organic residues preserved in Iron age lamps excavated at the site of Sahab in Jordan. Archaeometry 59 (5), 934–948. https://doi.org/10.1111/arcm.12288.
Meighan, C.W., Pendergast, D.M., Swartz, B.K., Wissler, M.D., 1958. Ecological interpretation in archaeology: part II. Am. Antiq. 24 (2), 131–150. https://doi.org/10.2307/277475.
Mileto, S., Kaiser, E., Rassamakin, Y., Evershed, R.P., 2017. New insights into the subsistence economy of the Eneolithic Dereivka culture of the Ukrainian North-Pontic region through lipid residues analysis of pottery vessels. J. Archaeol. Sci. Rep. 13, 67–74. https://doi.org/10.1016/j.jasrep.2017.03.028.
Morgado, A., Pelegrin, J., 2012. Origin and development of blade pressure production at the south of the Iberian Peninsula (ca. VIth–IIIrd millennium BC). In: Desrosiers, P.M. (Ed.), The Emergence of Pressure Blade Making. From Origin to Modern Experimentation. Springer, New York, pp. 219–235.
Mottram, H., Dudd, S., Lawrence, G., Stott, A., Evershed, R.P., 1999. New chromatographic, mass spectrometric and stable isotope approaches to the classification of degraded animal fats preserved in archaeological pottery. J. Chromatogr. A 833 (2), 209–221. https://doi.org/10.1016/S0021-9673(98)01041-3.
Parras, D.J., Sánchez, A., Tuñón, J.A., Rueda, C., Ramos, N., García-Reyes, J.F., 2015. Sulphur, fats and beeswax in the Iberian rites of the sanctuary of the oppidum of Puente Tablas (Jaén, Spain). J. Archaeol. Sci. Rep. 4, 510–524. https://doi.org/10.1016/j.jasrep.2015.10.010.
Prieto, M.P., Tresserras, J., Matamala, J.C., 2005. Ceramic production in the North-Western Iberian Peninsula: studying the functional features of pottery by analyzing organic material. In: Prudêncio, M.I., Dias, M.I., Waerenborgh, J.C. (Eds.), Understanding People through their Pottery. Proceedings of the 7th European Meeting on Ancient Ceramics (EMAC'03). October 27–31, 2003. 42. Instituto Tecnológico e Nuclear, Lisbon, Portugal, pp. 193–200 Lisboa: Instituto Português de Arqueologia Série Monográfica. Trabalhos de Arqueología.
Reber, E.A., Kerr, M.T., Whelton, H.L., Evershed, R.P., 2018. Lipid residues from low-fired pottery. Archaeometry 61 (1), 131–144. https://doi.org/10.1111/arcm.12403.
Regert, M., Colinart, S., Degrand, L., Decavallas, O., 2001. Chemical alteration and use of beeswax through time: accelerated ageing tests and analysis of archaeological samples from various environmental contexts. Archaeometry 43 (4), 549–556. https://doi.org/10.1111/1475-4754.00036.
Rice, P.M., 2015. Pottery Analysis: A Sourcebook. University of Chicago Press.
Roffet-Salque, M., Regert, M., Evershed, R.P., Outram, A.K., Cramp, L.J.E., Decavallas, O., Dunne, J., Gerbault, P., Mileto, S., Mirabaud, S., Pääkkönen, M., Smyth, J., Šoberl, L., Whelton, H.L., Alday-Ruiz, A., Asplund, H., Bartkowiak, M., Bayer-Niemeier, E., Belhouchet, L., Bernardini, F., Budja, M., Cooney, G., Cubas, M., Danaher, E.M., Diniz, M., Domboróczki, L., Fabbri, C., González-Urquijo, J.E., Guilaine, J., Hachi, S., Hartwell, B.N., Hofmann, D., Hohle, I., Ibáñez, J.J., Karul, N., Kherbouche, F., Kiely, J., Kotsakis, K., Lueth, F., Mallory, J.P., Manen, C., Marciniak, A., Maurice-Chabard, B., Mc Gonigle, M.A., Mulazzani, S., Özdoğan, M., Perić, O.S., Perić, S.R., Petrasch, J., Pétrequin, A.M., Pétrequin, P., Poensgen, U., Pollard, F., Poplin, C.J., Radi, G., Stadler, P., Stäuble, H., Tasić, N., Urem-Kotsou, D., Vuković, J.B., Walsh, F., Whittle, A., Wolfram, S., Zapata-Peña, L., Zoughlami, J., 2015. Widespread exploitation of the honeybee by early Neolithic farmers. Nature 527, 226–230. https://doi.org/10.1038/nature15757.
Roffet-Salque, M., Dunne, J., Altoft, D.T., Casanova, E., Cramp, L.J., Smyth, J., Whelton, Evershed, R.P., 2017. From the inside out: upscaling organic residue analyses of archaeological ceramics. J. Archaeol. Sci. Rep. 16, 627–640. https://doi.org/10.1016/j.jasrep.2016.04.005.
Rogge, W.F., Hildemann, L.M., Mazurek, M.A., Cass, G.R., Simoneit, B.R., 1991. Sources of fine organic aerosol. 1. Charbroilers and meat cooking operations. Environ. Sci. Technol. 25 (6), 1112–1125. https://doi.org/10.1021/es00018a015.
Rojo, M.A., Garrido, R., García, I., 2008. No sólo cerveza. Nuevos tipos de bebidas alcohólicas identificados en análisis de contenidos de cerámicas campaniformes del Valle de Ambrona (Soria). Cuadernos de Prehistoria de la Universidad de Granada 18. pp. 91–105.
Saliu-Modugno, F., Orlandi, M., Colombini, M.P., 2011. HPLC–APCI-MS analysis of triacylglycerols (TAGs) in historical pharmaceutical ointments from the eighteenth century. Anal. Bioanal. Chem. 401 (6), 1785–1800. https://doi.org/10.1007/s00216-011-5179-9.
Salque, M., Bogucki, P.I., Pyzel, J., Sobkowiak-Tabaka, I., Grygiel, R., Szmyt, M., Evershed, R.P., 2013. Earliest evidence for cheese making in the sixth millennium BC in northern Europe. Nature 493, 522–525. https://doi.org/10.1038/nature11698.
Sánchez, A., Cañabate, M.L., Lizcano, R., 1998. Archaeological and chemical research on sediments and ceramics at Polideportivo (Spain): an integrated approach. Archaeometry 40 (2), 341–350. https://doi.org/10.1111/j.1475-4754.1998.tb00842.x.
Simoneit, B.R.T., Rushdi, A.I., Abas, M.R.B., Didyk, B.M., 2003. Alkyl amides and nitriles as novel tracers for biomass burning. Environ. Sci. Technol. 37, 16–21. https://doi.org/10.1021/es020811y.
Smyth, J., Evershed, R.P., 2015. The molecules of meals: new insight into Neolithic foodways. Proc. R. Ir. Acad. Sect. C 115C (1), 1–20. https://doi.org/10.3318/priac.2015.115.07. 27.
Spangenberg, J.E., Jacomet, S., Schibler, J., 2006. Chemical analyses of organic residues

in archaeological pottery from Arbon Bleiche 3, Switzerland–evidence for dairying in the late Neolithic. J. Archaeol. Sci. 33 (1), 1–13. https://doi.org/10.1016/j.jas.2005.05.013.

Tuñón-López, J.A., Beneito-Cambra, M., Robles-Molina, J., Parras-Guijarro, D.J., Molina-Díaz, A., Sánchez-Vizcaíno, A., García-Reyes, J.F., 2017. Multiclass profiling of lipids of archaeological interest by ultra-high-pressure liquid chromatography-atmospheric pressure chemical ionization-high resolution mass spectrometry. Microchem. J. 132, 49–58. https://doi.org/10.1016/j.microc.2016.12.023.

Vera, J.C. (Ed.), 2014. Dossier. La Cueva de los Cuarenta (Priego de Córdoba). Avance a los resultados de la Intervención Arqueológica de 2007. Antiquitas 26, 71–133 coord.

Vigne, J.D., Helmer, D., 2007. Was milk a “secondary product” in the Old World neolithization process? Its role in the domestication of cattle, sheep and goats. Anthropozoologica 42 (2), 9–40.

Wang, J., Simoneit, B.R., Sheng, G., Chen, L., Xu, L., Wang, X., Wang, Y., Sun, L., 2017. The potential of alkyl amides as novel biomarkers and their application to paleo-cultural deposits in China. Sci. Rep. 7 (1), 14667. https://doi.org/10.1038/s41598-017-15371-z.

Zang, X., van Heemst, J.D., Dria, K.J., Hatcher, P.G., 2000. Encapsulation of protein in humic acid from a histosol as an explanation for the occurrence of organic nitrogen in soil and sediment. Org. Geochem. 31 (7–8), 679–695. https://doi.org/10.1016/S0146-6380(00)00040-1.